(c)2001 American Institute of Aeronautics & Astronautics or Published with Permission of Author(s) and/or Author(s)' Sponsoring Organization.

A01-16082

AIAA 2001-0161
Steady-State Wall Interference of a Symmetric Half-Model in the Langley Transonic Dynamics Tunnel (Invited – 1/2 hour)

A. J. Krynytzky

The Boeing Company

39th AIAA Aerospace Sciences Meeting and Exhibit

8-11 January 2001
Reno, Nevada

For permission to copy or republish, contact the American Institute of Aeronautics and Astronautics
1801 Alexander Bell Drive, Suite 500, Reston, VA 20191

(c)2001 American Institute of Aeronautics & Astronautics or Published with Permission of Author(s) and/or Author(s)' Sponsoring Organization.

AIAA 2001-0161

Steady-State Wall Interference of a Symmetric Half-Model in the Langley Transonic Dynamics Tunnel

A. J. Krynytzky*
Aerodynamics/Noise/Propulsion Laboratory
The Boeing Company
Seattle, WA

Abstract

A symmetric wing-body half-model was tested in the NASA Langley Transonic Dynamics Tunnel to determine basic tunnel upflow and wall interference characteristics. Wall interference of the slotted walls is determined experimentally from lift-curve slope comparisons between open and closed wall slots. Wall interference corrections for closed slots were computed using Tranair. The uncertainty of the lift interference parameter (δ_0) for open slots is estimated. Tranair calculations were also done for open slots. Measured wall pressures were used to guide the specification of the slotted wall boundary condition. These calculations serve as an independent check of the wall interference derived experimentally.

Introduction

Results of a cooperative Boeing-NASA test in the NASA Langley Transonic Dynamics Tunnel (TDT) are reported. This is the first of three tests supporting a BCAG (Boeing Commercial Airplane Group) program, Validation of Unsteady Aerodynamic Prediction Methods for Flutter and Dynamic Loads. The main thrust of this program is to validate a method for predicting the unsteady aerodynamics of subsonic transport aircraft. One of the key aerodynamic parameters from the standpoint of loads and flutter is lift-curve slope. Because the angle of attack correction due to wall interference directly affects lift-curve slope, this test focused on determining upflow and wall interference characteristics of the TDT using a symmetric wing-body half model.

Upflow is inferred from the model angle at zero lift. For a symmetric model this is the negative of the upflow. Wall interference characteristics are estimated using two independent methodologies: lift-curve slope comparisons to fully-corrected closed-wall slopes and computational fluid dynamics (CFD) calculations using a model of the slotted tunnel walls which is validated using wall pressures measured in this test.

Model Description

The calibration model is shown in the TDT test section in Figure 1. It is a 0.14 scale half-model of a wide-bodied product development study airplane of the late 1980's, Figure 2. Because of its intended use as a calibration model, the body is axisymmetric with an ellipsoidal nose and an ogive aft body with no upsweep. The wing is symmetric (no camber) and is centrally mounted between the fuselage crown and keel with zero dihedral. The trapezoidal wing planform has a quarter-chord sweep of 27.6 deg and an aspect ratio of about 9.5. The thickness and camber differ from others of the product development family because this wing was designed for a relatively high drag-rise Mach number and for zero lift at zero angle of attack. The model wing span of 100.8 in corresponds to a span to tunnel width ratio of 0.525 in the TDT.

Trip strips for initiating boundary layer transition were installed on the upper and lower surfaces of the wing at 10% local chord. The trip strip consisted of epoxy trip discs sized for the lowest test Reynolds numbers. The target trip height was 0.027 in. Pre-test trip height measurements varied from 0.025 to 0.028 in with a standard

---

* Senior Specialist Engineer, Member AIAA

Copyright © 2001 by The Boeing Company.
Published by the American Institute of Aeronautics and Astronautics, Inc. with permission.

(c)2001 American Institute of Aeronautics & Astronautics or Published with Permission of Author(s) and/or Author(s)' Sponsoring Organization.

deviation less than 0.001 in. A body nose trip strip was installed 4 in from the nose (measured along the body surface).

The wing has 8 streamwise rows of upper and lower surface pressures, with 34 pressure taps at each section. The model forces were measured using a five-component external strain gage balance provided by NASA, designated 1637S which has a normal force design load of 5700 lbs. The installed model weight was 3500 lbs.

Tunnel Description and Instrumentation

The NASA Langley TDT is a transonic sub-atmospheric pressure tunnel with the capability to test with either air or R134a as a test gas, reference 1. The conditions for this test are indicated on the R134a tunnel test envelope, Figure 3. These include Mach numbers (M) from 0.4 to 0.95 at target dynamic pressures (Q) of 75, 150, and 300 psf. The test section wall configurations included both open slots (see below) and closed slots (slot covers installed in all slots to provide a closed-wall test section). One Mach series with open slots was run in air at Q=150 psf.

The model was mounted on the east sidewall on tunnel centerline with the reference wing station at tunnel station STA 72 (STA units are ft). The test section has three longitudinal slots in each of the floor and ceiling with an openness ratio of 2.1 percent (based on test section perimeter). Each sidewall has two slots adding 2.2 percent to the net wall opennes. For this test the slots on the east sidewall had slot covers installed to simulate the aerodynamic plane of symmetry for a half model. The net slot openness for this half-model test is thus about 4.0 percent.

Six 12-ft static pressure rails were installed to measure wall pressure distributions. Existing wall static taps in the walls were also used. Wall pressure measurement locations are shown in Figure 4.

Clear Tunnel Calibration

Clear test section calibration runs preceded model testing. A 5-hole calibration probe known as Superprobe II was mounted to the pitch strut with the probe static pressure taps located at STA 72 on tunnel centerline, see Figure 4.

Mach number in the TDT slotted test section is calculated from two pressure measurements: static pressure in the test section plenum remote from the test section walls, and total pressure using a pitot tube on the sidewall of the settling chamber upstream of the test section. For closed-wall testing the west sidewall static pressure tap at STA 45 was used as the static reference source for test section Mach number control and calculation. These pressures are correlated to corresponding probe pressures at the model location in the test section. Calibration runs determine calibration pressure ratios PSCORR and PTCORR so that corrected pressures in the test section are given by:

$$PS_c = PS_{unc}(PSCORR) \qquad (1)$$

$$PT_c = PT_{unc}(PTCORR) \qquad (2)$$

where PS and PT are static and total pressure respectively; subscripts c and unc designate corrected (i.e. from Superprobe II) and uncorrected pressures. PSCORR and PTCORR are determined as functions of Mach number and dynamic pressure. A pressure correction of 0.1% (i.e., PSCORR or PTCORR = 1.001) corresponds to a Mach number correction of about 0.001 for Mach numbers above 0.7.

The pressure calibrations for open and closed slots are shown in Figure 5. In the slotted test section the static pressure correction ratio is near 1.0 (Fig 5a), consistent with experience in test sections with ventilated walls which are surrounded by a large plenum chamber. This correction does not appear to vary significantly with Reynolds number (i.e., Q and M). The apparent step in the calibration characteristics between M=0.85 and 0.88 is thought to be due to a re-entry door schedule change between these conditions. These data are consistent with unpublished static pipe measurements for the slotted test section which indicate only very small static pressure differences at the model reference station relative to plenum pressure. Total pressure corrections (Fig 5c) also appear to be very small, except at the lowest Q.

For open slots, no static pressure corrections were applied, even though the step between M=0.85 and 0.88 seems to capture the effect of

(c)2001 American Institute of Aeronautics & Astronautics or Published with Permission of Author(s) and/or Author(s)' Sponsoring Organization.

the re-entry door change at an incremental level of about 0.2%.

For closed slots, if the walls do not leak, the static pressure correction (Fig 5b) will depend only on wall divergence (which is fixed) and on wall boundary layer growth which may vary with Reynolds number. A pressure ratio near 1.0 suggests a wall divergence angle matched to the average rate of boundary layer growth. This is the case for Q=150 psf. At Q=75 psf, excess wall boundary layer growth occurs resulting in an increased test section Mach number relative to upstream. At this Q, pressure ratios above M=0.85 appear to be shifted relative to the trend at lower Mach numbers. Although this characteristic is similar to the re-entry door effect noted above for the slotted test section, door instrumentation confirms fixed door positions through the entire Mach range (as was intended for closed slot testing). At Q=300 psf the increased static pressure at the calibration location indicates excess wall divergence.

For closed slots the static pressure corrections were curve-fit with the exception of the anomaly at Q=75 psf above M=0.85. These conditions have the lowest tunnel total pressure, about 250 psf, and therefore data accuracy may be expected to suffer from an instrumentation standpoint because of the small pressure differences being measured. The Superprobe II data clearly show increased data scatter at these lowest pressure conditions. The smooth behavior of the static pressure correction at Q=150 and 300 psf supports a similar expectation at Q=75 psf. These two considerations contribute to the judgement that the low Q data are suspect. The calibration at Q=75 psf is therefore based on an extrapolation of the fit from low Mach numbers based on similar monotonicity as at higher Q's.

No total pressure corrections were used for either closed or open slots. Even though data for both wall configurations show similar trends with both Mach number and Q (Fig 5c and 5d), the magnitudes of these variations are different. Based on similar measurements in the Boeing Transonic Wind Tunnel (BTWT) better correspondence between these data sets was expected. However, it is not known which (if either) data set is more accurate.

These probe static and total pressure measurements provide a basis for estimating calibration contributions to Mach number uncertainty. The bias uncertainty (at 95% confidence) for each of these corrections is taken to be 0.25% based on the range of probe measurements. This corresponds to a Mach number uncertainty of about 0.005 for each correction, or about 0.007 for both uncertainties summed in a root-sum-squares (RSS) sense.

An additional source of uncertainty of Mach number at the model location is the unknown variation of Mach number (total and static pressure) throughout the volume occupied by the model wing. No estimate of the magnitude of the pressure variations was made. Flow surveys of the test section are recommended to quantify these effects.

Closed Slots Wall Interference Corrections

The wall interference of the TDT closed walls on the wing-body half model was computed using Tranair, reference 2. The model and tunnel paneling are shown in Figure 6.

The methodology for calculating wind tunnel wall interference is analogous to potential flow panel methods, references 3 and 4. As long as the flow is subsonic at the walls this approach includes the additional interference due to local regions of supersonic flow near the model. Streamwise interference velocities were evaluated at the 0.25 chord of the wing mean aerodynamic chord (MAC), located at wing buttock line (WBL) 40.14. The upwash interference velocities were evaluated at the 0.75 MAC. These interference estimates for closed walls are summarized in Figure 7.

Tranair blockage results closely track classical linear wall interference predictions up to about M=0.85 (Fig 7a). For lift interference (Fig 7b), classical linear theory suggests a value of 0.098 for δ_0, independent of Mach number. A slightly higher value, 0.105, is found by extrapolating the calculated results in reference 3.

These closed wall corrections were applied to the closed slots force data, resulting in an interference-free dataset.

(c)2001 American Institute of Aeronautics & Astronautics or Published with Permission of Author(s) and/or Author(s)' Sponsoring Organization.

Open Slots Wall Interference Calculations

Initial Tranair calculations of open slots interference are also shown in Figure 7. The tunnel walls were modeled as alternating closed-wall segments (slats) and open-wall segments (slots) corresponding to the actual tunnel wall geometry. The ideal porous wall boundary condition was applied at the slots:

$$R\varphi_x + \varphi_n = 0 \qquad (3)$$

where φ is the perturbation velocity potential; x and n denote derivatives in the streamwise and normal (to the wall) directions, and R is the porous wall permeability factor. This boundary condition specifies the velocity through the slots to be directly proportional to the pressure difference across the test section wall. R=0 corresponds to a closed wall; R very large corresponds to a constant pressure boundary. A nominal value of this factor consistent with experience with other slotted tunnels (mainly BTWT and the Ames 11-ft, ref 5) was used in the initial calculations: R=18.

This slotted wall model is the starting point for development and validation of a computational model of the tunnel by providing predicted wall pressures for comparison to measured wall pressures. Variation of the wall permeability (R) is the primary degree of freedom for converging to a computational wall model.

Model Lift

Measured model lift curves in R134a for closed and open slots are compared in Figure 8. Closed slots data include clear test section static pressure calibration factors and solid blockage and upwash interference corrections. Open slots data are uncorrected for these items.

Lift curves compare very well at low Mach numbers with regard to both slope and offset. At Q=150 psf noticeable deviations start at M=0.85 at lift levels above the slope break. At Q=300 and 75 psf small differences in lift-curve slope are apparent even at low Mach numbers, with larger differences appearing at higher Mach numbers and lift levels, especially for Q=75 psf.

Tunnel upflow is estimated assuming the model is aerodynamically symmetrical; with no upflow, the lift curve should intercept the axis origin (α=0 at C_L=0). The measured lift-curve intercept is then the negative of the upflow. The lift-curve slope is evaluated for $-0.25 \leq C_L \leq +0.25$. Upflow and slope comparisons with closed and open slots are shown in Figure 9. It is concluded that within the accuracy of these data, there are no variations of upflow with either M or Q. Upflow with open slots is approximately -0.02 deg (±~0.02 deg). Tunnel upflow with closed slots appears to be about -0.04 deg.

The fully-corrected closed slots force data provide the baseline for estimating slotted wall lift interference. However, this baseline becomes less trustworthy with increasing Mach number as supersonic flow regions around the model increase in extent. Assuming that the solid blockage of the slotted walls is negligible, lift interference for open slots can be directly determined from the required correction to lift-curve slope.

At Q=150 psf, the lift-curve slope comparisons up to M=0.85 are very close for open and closed slots. At Q=300 psf, open slot slopes are somewhat smaller than closed slot slopes. A small negative correction (for the open slots) would be required to collapse these slopes. The slopes at Q=75 psf also correspond well; a very small positive α-correction to the open slots data (0.40<M<0.88) would bring the lift curves into consonance.

Thirteen sets of repeat runs (with 3-5 runs per set; 46 runs total) were used to estimate the experimental precision of the lift-curve slopes. The standard deviation (prediction interval) of the slope is estimated from the median absolute deviation of each run's slope from the (appropriate) average to be about 0.00068 (per degree). This assumes similar uncertainty at all dynamic pressures. Deletion of the worst two outliers significantly decreases the estimated standard deviation to about 0.00045. This latter value will be used in the uncertainty analysis of lift interference. It corresponds to a lift-curve slope uncertainty (at 95% confidence) of 0.6-0.9%, depending on Mach number and Q.

Lift interference of Slotted Walls

The corrected lift-curve slope for a model in a wind tunnel can be calculated from the

(c)2001 American Institute of Aeronautics & Astronautics or Published with Permission of Author(s) and/or Author(s)' Sponsoring Organization.

uncorrected (measured) lift-curve slope if the wall interference parameters are known,

$$\frac{1}{a_c} = \frac{1}{a_{unc}}\left(\frac{q_c}{q_{unc}}\right) + \frac{180}{\pi}\frac{S}{C}\delta_0 \qquad (4)$$

where a = lift-curve slope
q = dynamic pressure=1/2 ρ V^2
S = wing area=14.769 ft^2
C = tunnel area=248 ft^2
δ_0 = lift interference parameter
subscript c = corrected
subscript unc = uncorrected (i.e., measured).

The last term in (4) is the angle of attack correction per C_L (in degrees) due to the walls.

Lift interference in the slotted tunnel can be calculated from application of equation (4) for both closed slots and for open slots; the assumption being that fully-corrected lift-curves should be the same regardless of test section. Equating the corrected lift-curve slopes from each test section (eq. 4) and solving for δ_0 for open slots,

$$\delta_{0_{OS}} = \frac{\pi}{180}\frac{C}{S}\frac{1}{a_{unc_{CS}}}\left(\frac{q_c}{q_{unc}}\right)_{CS} + \delta_{0_{CS}} - \frac{\pi}{180}\frac{C}{S}\frac{1}{a_{unc_{OS}}}\left(\frac{q_c}{q_{unc}}\right)_{OS} \qquad (5)$$

where the subscripts OS and CS denote open slots and closed slots, respectively.

The corrected lift-curve slope at a given M and Q is calculated from the closed slots data using blockage and lift interference corrections from the Tranair analyses. For slotted wall data, it is assumed that solid blockage is negligible. Figure 10 compares the derived lift interference at each Q to the CFD results of Figure 7. The results are centered near δ_0 = 0 at Mach numbers up to 0.85, with large variations at M=0.88. The apparent variation of wall interference with Q must be evaluated critically with respect to overall uncertainty.

Uncertainty of Lift Interference

The uncertainty analysis of lift interference presented here relies on standard uncertainty analysis techniques: root-sum squares of uncertainty sources. Simple in principle, the application of uncertainty estimation techniques is surprisingly infrequent.

In equation 5, each of the q ratios can be considered the product of three factors representing clear tunnel static and total pressure calibrations, and solid blockage of the model. Ignoring the wing and test section areas (C and S) contributions to the uncertainty, this leaves nine variables contributing to the uncertainty of lift interference in the open slots test section ($\delta_{0,OS}$):

1. measured uncorrected lift-curve slope with closed slots ($a_{unc,CS}$)
2. estimated (CFD) blockage with closed slots ($\varepsilon_{0,CS}$)
3. static pressure calibration with closed slots ($PSCORR_{CS}$)
4. total pressure calibration with closed slots ($PTCORR_{CS}$)
5. estimated lift interference with closed slots ($\delta_{0,CS}$)
6. measured uncorrected lift-curve slope with open slots ($a_{unc,OS}$)
7. estimated (CFD) blockage with open slots ($\varepsilon_{0,OS}$)
8. static pressure calibration with open slots ($PSCORR_{OS}$)
9. total pressure calibration with open slots ($PTCORR_{OS}$)

The solid blockage parameter, ε_0, is defined conventionally as

$$\varepsilon_0 = \frac{\Delta u_{sb}}{U_{unc}} \qquad (6)$$

where Δu_{sb} is the streamwise velocity correction due to model solid blockage and U_{unc} is uncorrected test section velocity. Corresponding Mach number and dynamic pressure corrections are given by the linear relationships (ref 6)

$$M_{corr} = M_{unc}\left[1 + \left(1 + \frac{\gamma - 1}{2}\right)M_{unc}^{\ 2}\varepsilon_0\right] \qquad (7)$$

$$q_{corr} = q_{unc}\left[1 + \left(2 - M_{unc}^{\ 2}\right)\varepsilon_0\right] \qquad (8)$$

where γ is the ratio of specific heats, nominally 1.13 for R134a.

The uncertainty of the above experimentally determined values of δ_0 for open slots is the root-

(c)2001 American Institute of Aeronautics & Astronautics or Published with Permission of Author(s) and/or Author(s)' Sponsoring Organization.

sum-square of at least these nine sources of uncertainty. There are two experimental uncertainties of measured lift-curve slopes (1 and 6), two uncertainties of CFD-estimated blockage (2 and 7), one uncertainty of CFD-estimated lift interference in the closed slots test section (5), and four calibration uncertainties (3,4,8,and 9). For the most part, the experimental repeatability of lift-curve slope may be viewed as random or "precision" uncertainties while the uncertainties due to clear test section calibration and due to CFD corrections may be viewed as systematic or "bias" uncertainties. These uncertainties are assumed to be uncorrelated.

The experimental repeatability of the lift-curve slopes is approximately 0.00045 (one sigma). Similar precision is assumed for each test section. The calibration uncertainties are taken at 0.25% (two sigma) for each pressure correction (see Figure 5). Lacking a rigorous approach to evaluating CFD uncertainties, the interference uncertainties (at 95% confidence) are taken to be the predicted variation of interference over the wing planform at M=0.80: about 0.0024 solid blockage variation ($\Delta\varepsilon_0$) and about 0.023 lift interference variation ($\Delta\delta_0$).

These levels of uncertainty and their contribution to uncertainty of the predicted δ_0 in the slotted test section with no repeat runs are shown in Figure 11. The RSS 95% uncertainty for δ_0 for this case is ±0.045. This corresponds to about 1.3-2.0% in model lift-curve slope, depending on Mach number.

Consideration of aggressive goals for decreasing uncertainties provides a best-case scenario as well as identifies the magnitude of reductions required to achieve a more accurate result. For example, N repeat runs in each test section decreases the uncertainty of the average measured lift-curve slope by $1/\sqrt{N}$. Figure 11 also shows the uncertainty for a case with four repeat runs in each test section, calibration uncertainties at 0.1%, and CFD uncertainties decreased by half. Uncertainty of δ_0 from this test is probably between these two estimates and almost certainly is no smaller than the lesser, 0.021.

Returning to the values of δ_0 derived from lift-curve slope comparisons, Figure 10, the indicated variation with Q covers a range not very different than ±0.045, the conservative (i.e., larger) estimate of δ_0 uncertainty. The large uncertainty relative to the differences with Q calls into question the accuracy of the indicated trend in Figure 10.

Wind Tunnel Wall Pressures, Open Slots

Pressures at the wind tunnel walls were measured to assist evaluation of the wall boundary condition, see Figure 4. Note that for the wall pressure plots, tunnel station (TSTA) is given in inches rather than the facility convention of feet (STA). Model center is TSTA 864 (STA 72).

With the model installed, wall pressures vary with model angle of attack, Figure 12. Only selected angles are plotted for clarity. An overall longitudinal pressure gradient due to the model (i.e., in addition to clear tunnel gradients) is observed. This characteristic of ventilated wall tunnels gives rise to a buoyancy force on the model, variously known as blockage buoyancy, buoyancy due to solid blockage gradients, or solid blockage induced buoyancy (SBIB). Variation of wall pressure with model lift is greatest near the model vertical plane of symmetry (the east tunnel sidewall). Model disturbance variation with angle of attack decreases to very small levels upstream of the model. The blockage signature of the model is apparent even far upstream of the model for the wall pressure rows nearest the model, but decreases to very small levels for the pressures away from the model (e.g., the upstream outboard ceiling and west wall pressures).

The utility of these pressures for validation of a computational model of the tunnel walls is enhanced by explicitly taking advantage of the regular variation of these pressures with model lift. This technique was developed by John Bussoletti for BTWT (see reference 4, chapter 3). For each run (i.e., angle of attack variation at constant Mach number and dynamic pressure) each individual wall pressure (the i-th pressure coefficient) is fit in a linear least-squares sense against model lift (C_L),

(c)2001 American Institute of Aeronautics & Astronautics or Published with Permission of Author(s) and/or Author(s)' Sponsoring Organization.

$$C_{p_i} = CF0_i + CF1_i \times C_L \qquad (9)$$

where $CF0_i$ and $CF1_i$ are coefficients of the least-squares fit. $CF0_i$ (intercept) is the pressure signature of the model at zero lift, and includes the clear tunnel wall pressure signature. As inspection of the data reveals, $CF0_i$ also includes the effect of pressure instrumentation zero shifts and offsets. $CF1_i$ (slope) is that part of the wall pressure signature due to model lift. The quality of a linear fit to the individual wall pressures deteriorates with increasing Mach number, especially with regard to fitting both positive and negative angles of attack due to compressibility effects.

Figures 13 and 14 show $CF0_i$ and $CF1_i$ respectively for open slots at M=0.70. Analogous results from fitting CFD wall pressures from runs at three angles of attack are shown for comparison. The CFD blockage signature in Figure 13, $CF0_i$, compares fairly well with the experimental pressures. It is expected that measured wall pressures downstream of the model would diverge from the CFD pressures because the tunnel diffuser and strut are not modeled in Tranair. The measured lift signature in Figure 14, $CF1_i$, compares very well with the CFD results. A variation of wall pressures with Reynolds number (Q) is not apparent from these data, countering the lift-curve slope results which show an apparent variation of interference with Q. Wall pressure comparisons at higher Mach numbers are worse with increasing Mach number. This is an area of continuing analysis. The fact that CFD predictions of lift interference are bracketed by the experimental results (Fig 10) lends credence to the CFD analysis. The CFD analysis, in turn, predicts very small blockage which supports the initial assumption of zero blockage in the slotted test section.

Conclusions

Clear tunnel static and total pressure calibration corrections for the open slots test section are small: of the order 0.25% or less. To obtain a Mach number accuracy of less than 0.002, static and total pressure calibrations must be determined to less than about 0.1%. Clear tunnel upflow is about -0.02 deg in the slotted test section.

Corrected model lift curves for closed slots compare well with (uncorrected) open slots lift curves up to M=0.80. The estimated prediction interval of the model's measured lift-curve slope is about 0.5% based on several sets of repeat runs.

In the slotted test section, lift interference (δ_0) uncertainty (at 95% confidence) is estimated to be 0.04 and 0.02 using conservative and aggressive values, respectively, for the component uncertainties. The corrected model lift-curve slope uncertainty corresponding to the conservative estimate of wall interference uncertainty is in the range of 1.3-2.0% depending on Mach number.

The indicated variation of lift interference with Q based on lift-curve slope comparisons between open and closed slots is about $\pm 0.05\ \delta_0$ at M=0.70. This spread is only slightly greater than the predicted uncertainty at 95% confidence. On the other hand, wall pressure data do not show variations with Q. The question of variation of wall characteristics with Q within the quoted uncertainty is not resolved.

The CFD (Tranair) model of the slotted walls does a credible job of predicting incremental wall pressures at M=0.7.

Based on the lift-curve slope results and the approximate, but as yet imperfect correlations of CFD and measured wall pressures, the apparent wall interference for this model in the TDT is small, for both lift and blockage interference for Mach numbers below 0.88. To decrease uncertainties associated with the lift-curve slope analysis, improvements are required in tunnel calibration corrections, in the use of repeat runs, and in increasing confidence in the computational interference results. The computational slotted wall model needs refinement in validation methodology using wall pressures, especially at high subsonic Mach numbers.

Acknowledgements

This work was performed under a cooperative agreement between the Boeing Company and the NASA Langley Research Center.

(c)2001 American Institute of Aeronautics & Astronautics or Published with Permission of Author(s) and/or Author(s)' Sponsoring Organization.

The Tranair CFD setup and calculations were done by John Bussoletti of Aerodynamics Tools, Methods, and Technology. Matt Smith contributed valuable trouble-shooting support. Mat Rueger and Mark Kammeyer of Boeing/St. Louis provided consultation on uncertainty analysis and helped lay the groundwork for this application.

References

1. "The Langley Transonic Dynamics Tunnel", LWP-799, Langley Research Center, September, 1969.
2. Johnson, F. T., Samant, S. S., Bieterman, M. B., Melvin, R. G., Young, D. P., Bussoletti, J. E., and Hilmes, C. G., "Tranair: A Full-Potential, Solution-Adaptive, Rectangular Grid Code for Predicting Subsonic, Transonic, and Supersonic Flows About Arbitrary Configurations", NASA CR 4348, December, 1992.
3. "Upwash interference for wings in solid-liner wind tunnels using subsonic linearised-theory", ESDU 95014, October, 1995.
4. "Wind Tunnel Wall Corrections", AGARDograph 336, edited by B. F. R. Ewald, October, 1998.
5. Goldhammer, M. E., and Steinle, F. W., Jr., "Design and Validation of Advanced Transonic Wings Using CFD and Very High Reynolds Number Wind Tunnel Testing", 17th ICAS Congress, September, 1990.
6. Pindzola, M., and Lo, C.F., "Boundary Interference at Subsonic Speed in Wind Tunnels with Ventilated Walls", AEDC-TR-69-47, May, 1969.

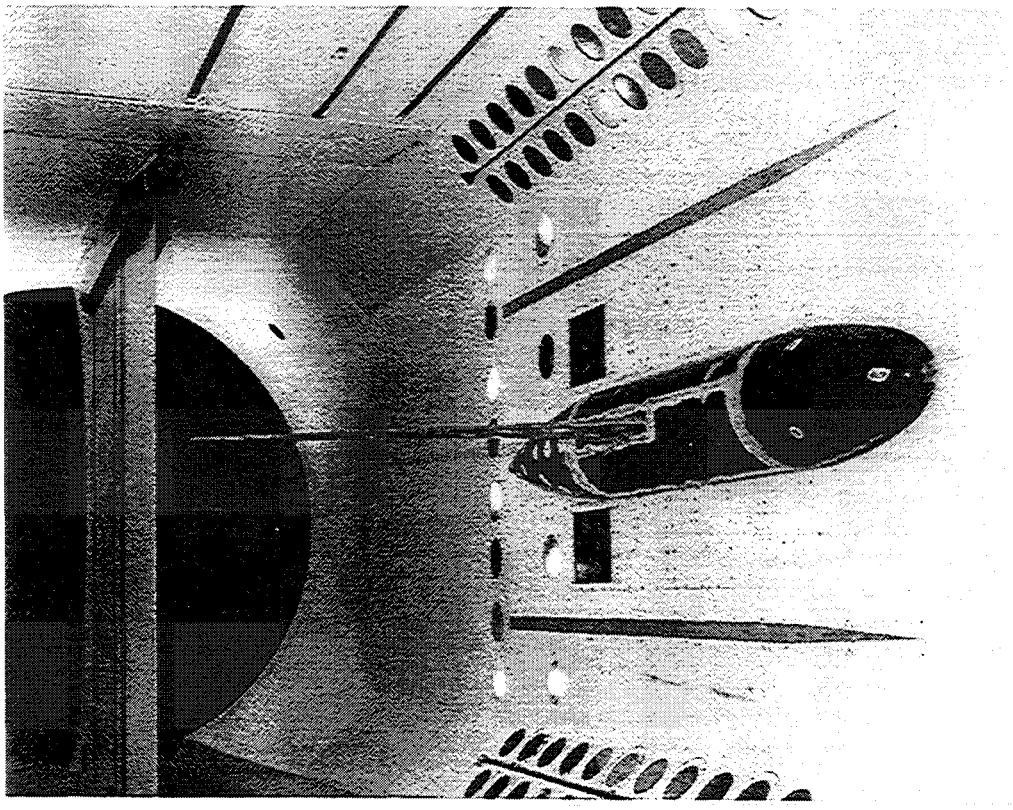

Figure 1 Symmetric Calibration Half Model in the NASA Langley Transonic Dynamics Tunnel

(c)2001 American Institute of Aeronautics & Astronautics or Published with Permission of Author(s) and/or Author(s)' Sponsoring Organization.

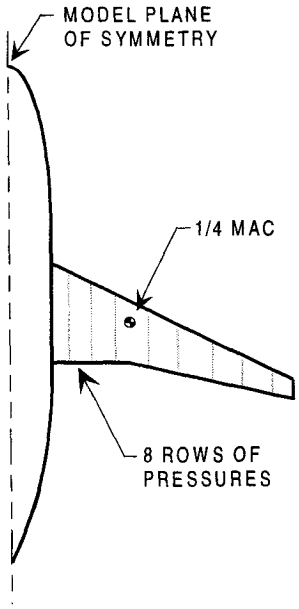

WING AREA	=	14.68 FT^2
SEMI-SPAN	=	100.8 IN
MAC	=	21.96 IN
ASPECT RATIO	=	9.56
TAPER RATIO	=	0.24
1/4 CHORD SWEEP	=	27.6 DEG
BODY LENGTH	=	199.4 IN
MAX BODY DIAMETER	=	26.3 IN

Figure 2 Symmetric Calibration Model Geometry

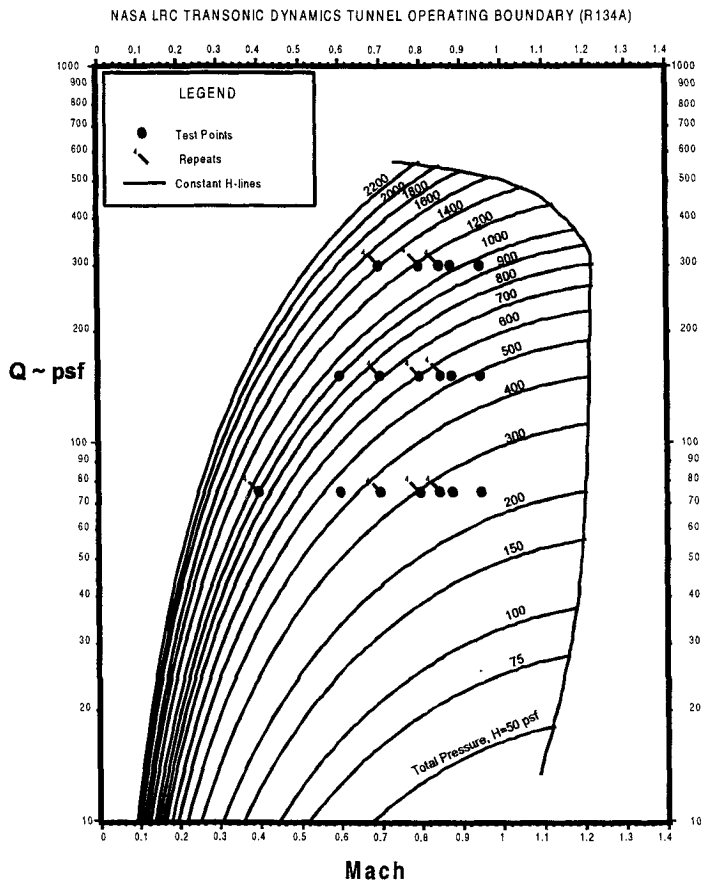

Figure 3 Test Conditions for Calibration Model in the TDT

(c)2001 American Institute of Aeronautics & Astronautics or Published with Permission of Author(s) and/or Author(s)' Sponsoring Organization.

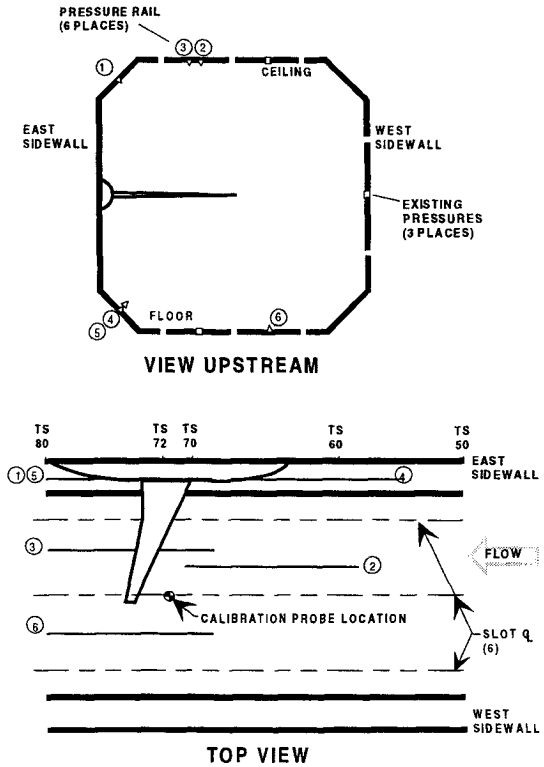

Figure 4 Calibration Model in TDT with Wall Pressures

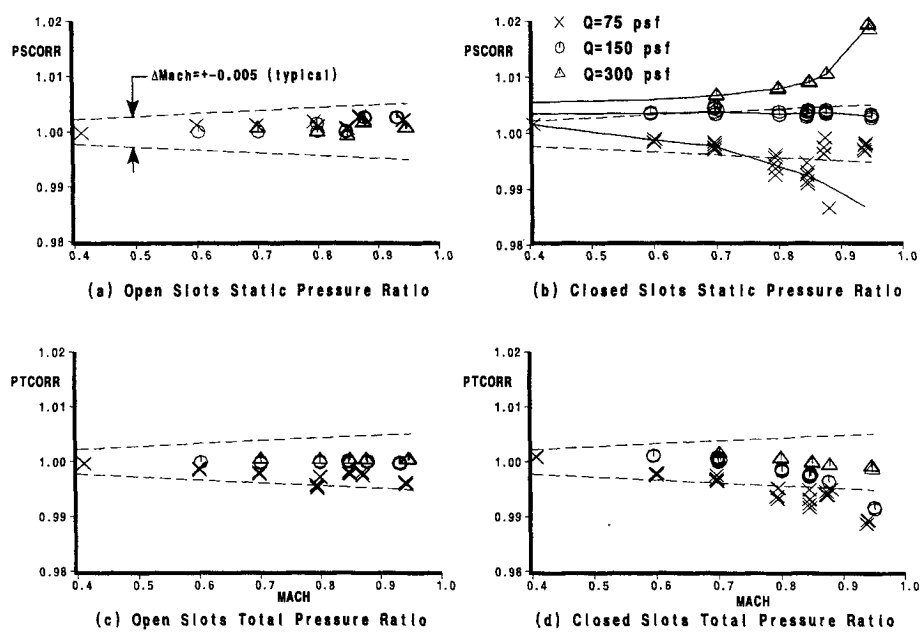

Figure 5 Clear Tunnel Pressure Calibration Factors

(c)2001 American Institute of Aeronautics & Astronautics or Published with Permission of Author(s) and/or Author(s)' Sponsoring Organization.

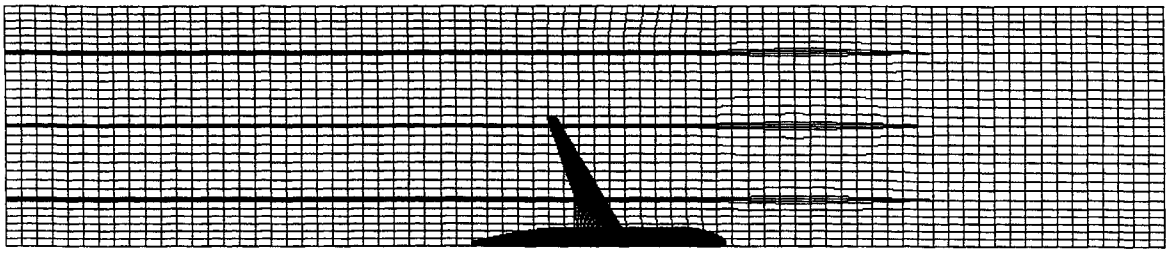

Figure 6 Tunnel and Model Paneling for Tranair

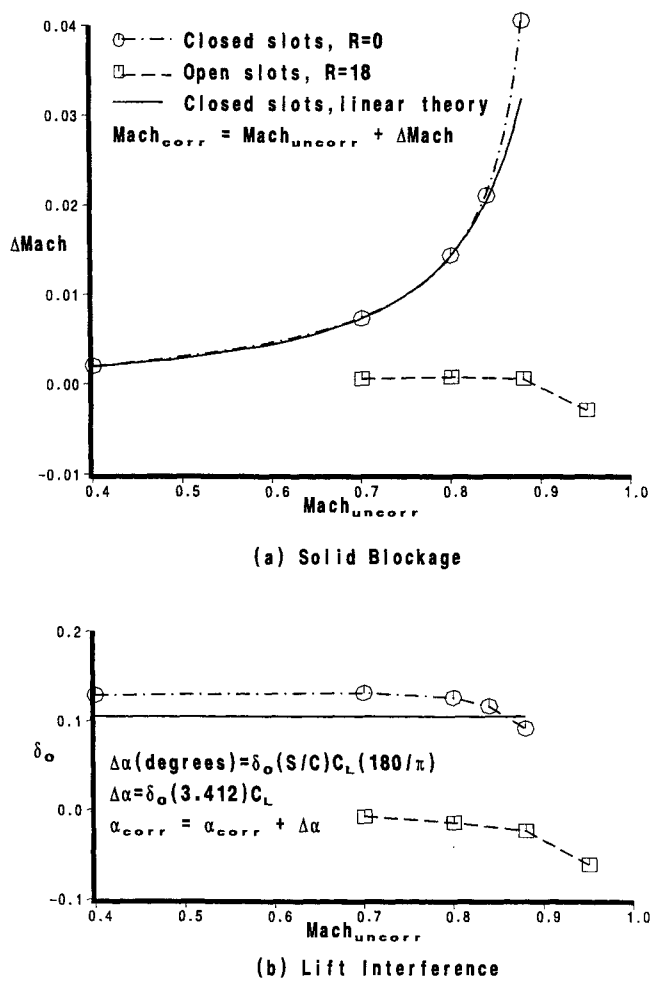

Figure 7 Tranair Estimates of Wall Interference

(c)2001 American Institute of Aeronautics & Astronautics or Published with Permission of Author(s) and/or Author(s)' Sponsoring Organization.

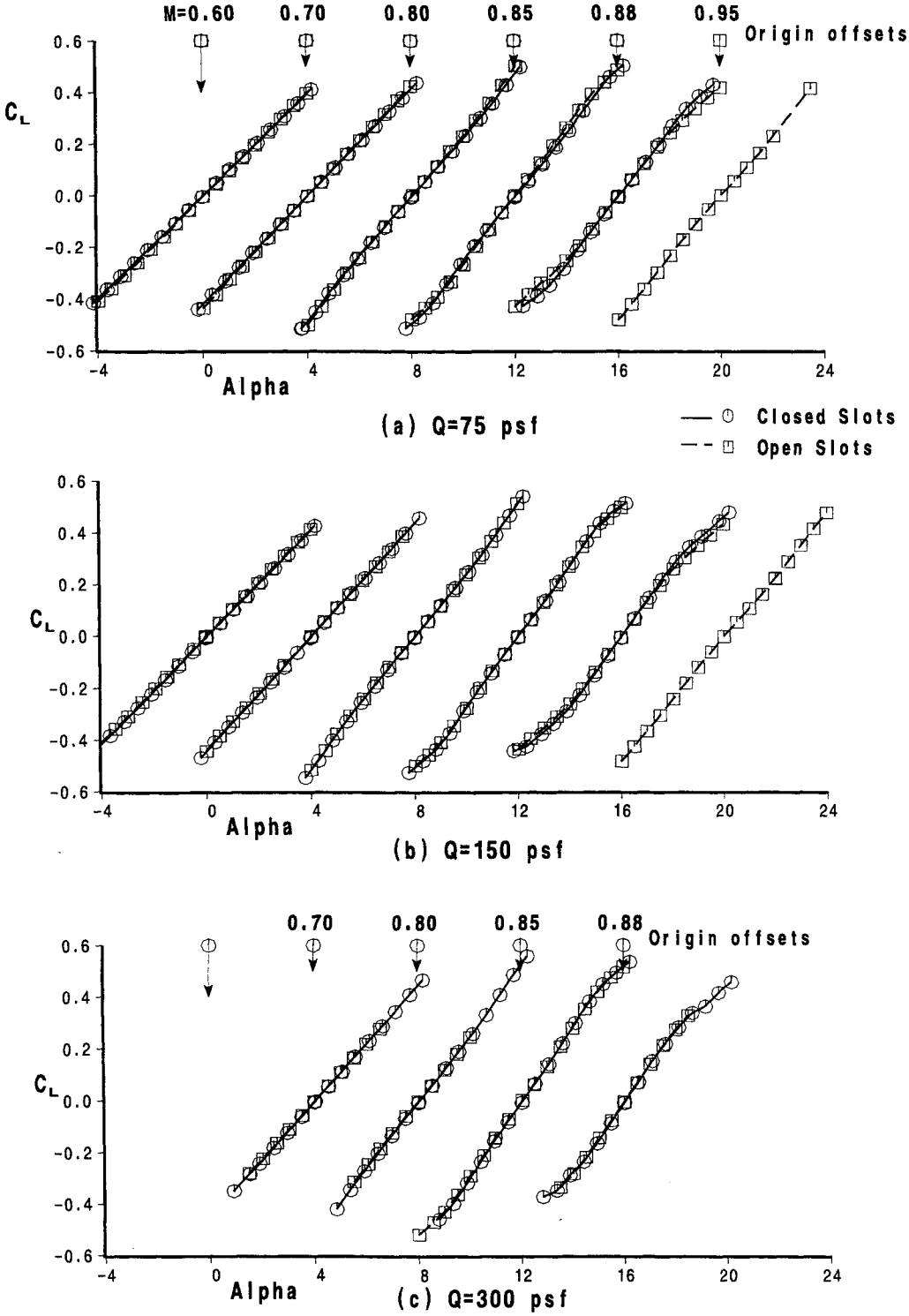

Figure 8 Model Lift Curves in R134a

(c)2001 American Institute of Aeronautics & Astronautics or Published with Permission of Author(s) and/or Author(s)' Sponsoring Organization.

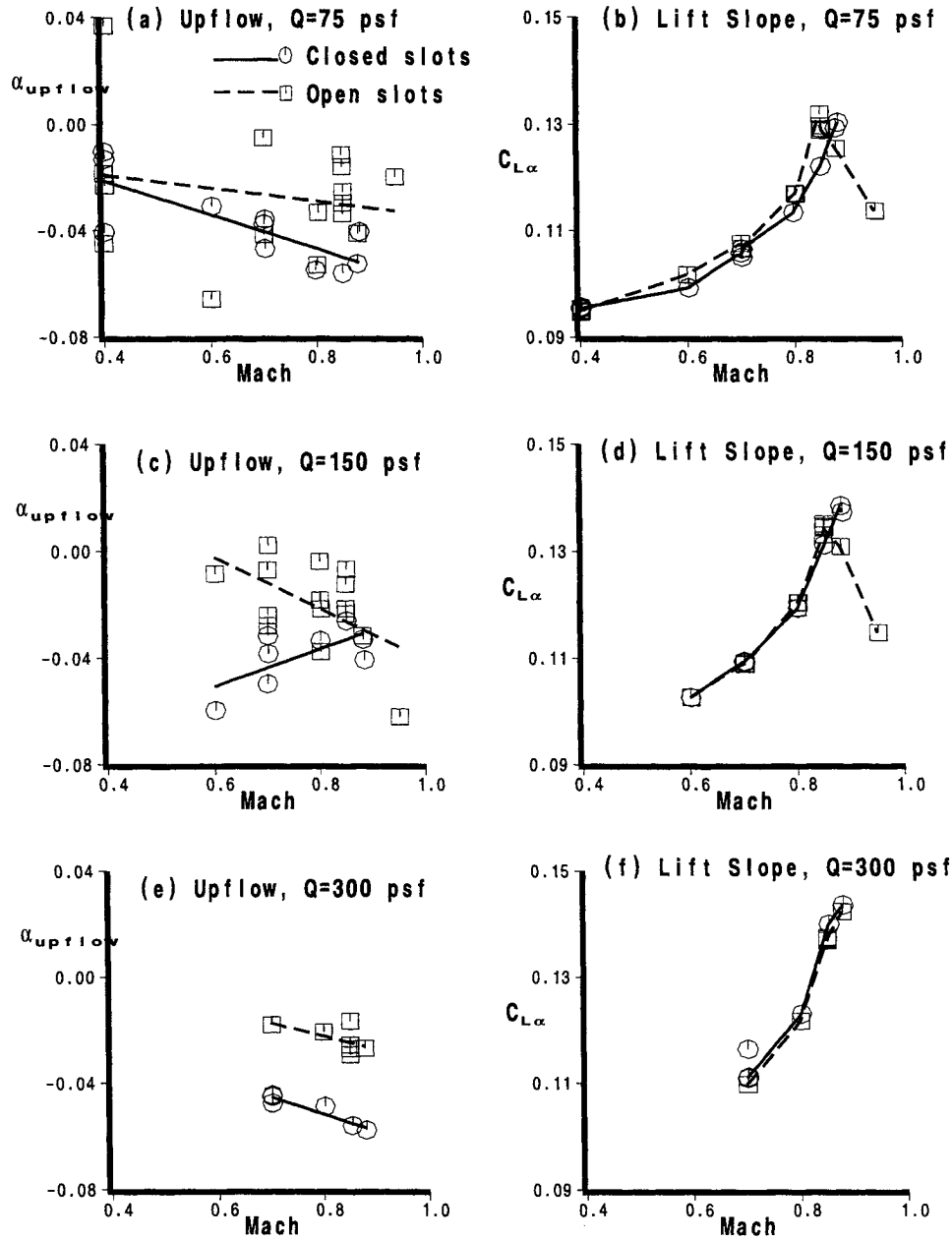

Figure 9 Upflow and Model Lift-Curve Slopes

(c)2001 American Institute of Aeronautics & Astronautics or Published with Permission of Author(s) and/or Author(s)' Sponsoring Organization.

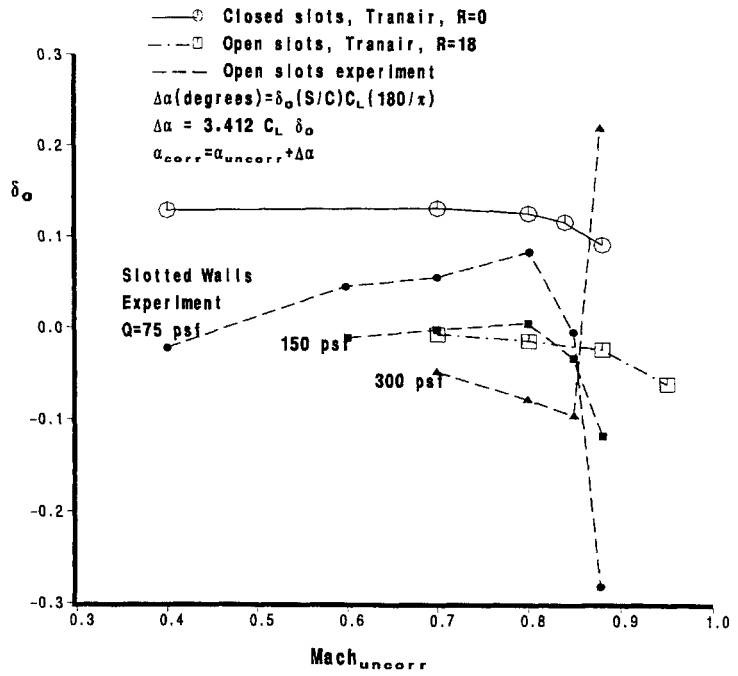

Figure 10 Lift Interference with Open Slots from Lift Curve Slope Comparisons

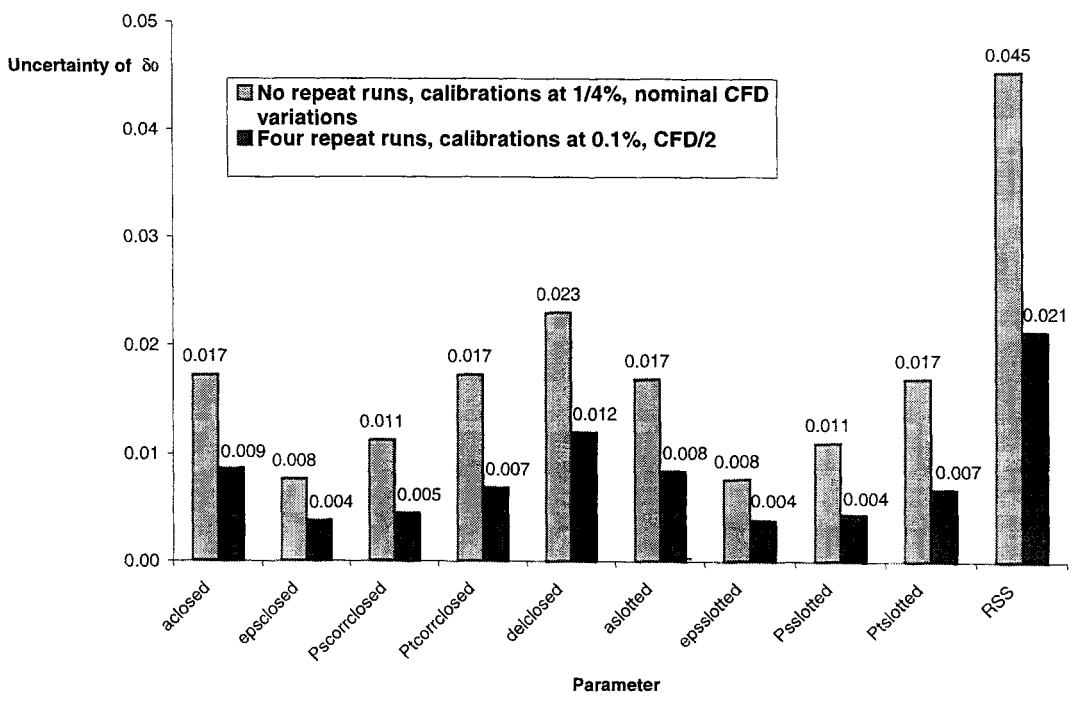

Figure 11 Uncertainty of Slotted Wall Lift Interference Parameter

(c)2001 American Institute of Aeronautics & Astronautics or Published with Permission of Author(s) and/or Author(s)' Sponsoring Organization.

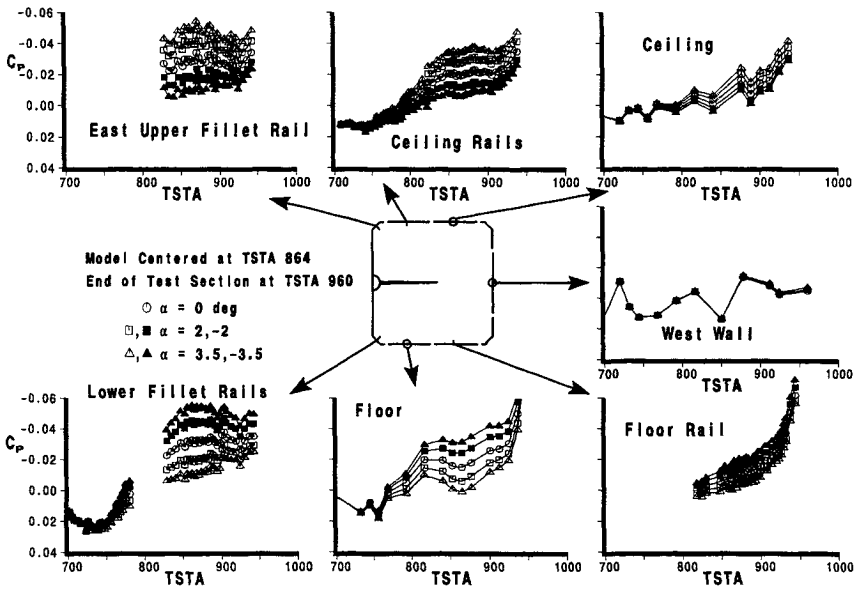

Figure 12 Open Slots Measured Wall Pressures, M=0.70, Q=150 psf

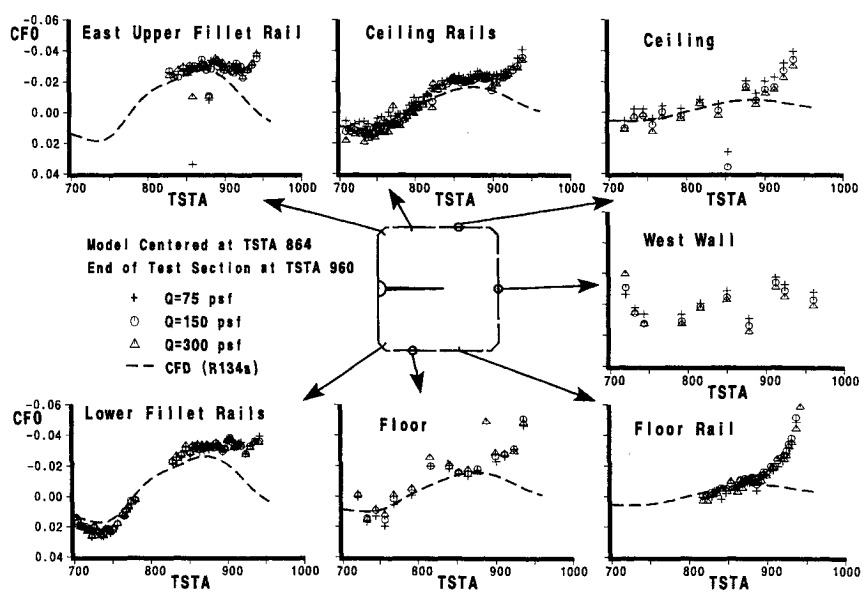

Figure 13 Wall Pressure Intercepts, Open Slots, M=0.70

(c)2001 American Institute of Aeronautics & Astronautics or Published with Permission of Author(s) and/or Author(s)' Sponsoring Organization.

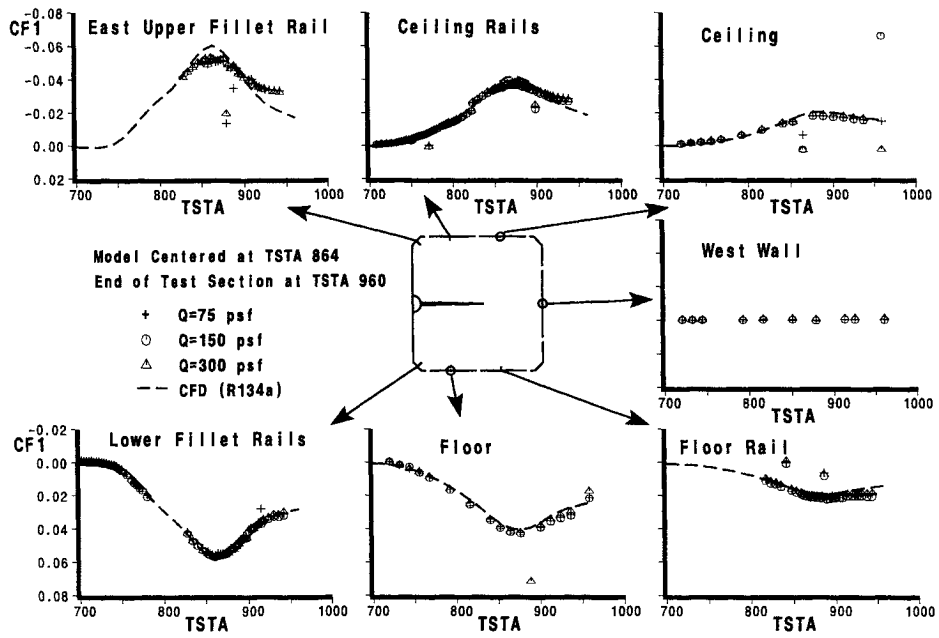

Figure 14 Wall Pressure Slopes, Open Slots, M=0.70